

An anisotropic, non-singular early universe model leading to a realistic cosmology

Pierre-Philippe Dechant,^{*} Anthony N. Lasenby,[†] and Michael P. Hobson[‡]

Astrophysics Group, Cavendish Laboratory,

J J Thomson Avenue, University of Cambridge, CB3 0HE, UK

(Dated: April 2, 2024)

Abstract

We present a novel cosmological model in which scalar field matter in a biaxial Bianchi IX geometry leads to a non-singular ‘pancaking’ solution: the hypersurface volume goes to zero instantaneously at the ‘Big Bang’, but all physical quantities, such as curvature invariants and the matter energy density remain finite, and continue smoothly through the Big Bang. We demonstrate that there exist geodesics extending through the Big Bang, but that there are also incomplete geodesics that spiral infinitely around a topologically closed spatial dimension at the Big Bang, rendering it, at worst, a quasi-regular singularity. The model is thus reminiscent of the Taub-NUT vacuum solution in that it has biaxial Bianchi IX geometry and its evolution exhibits a dimensionality reduction at a quasi-regular singularity; the two models are, however, rather different, as we will show in a future work. Here we concentrate on the cosmological implications of our model and show how the scalar field drives both isotropisation and inflation, thus raising the question of whether structure on the largest scales was laid down at a time when the universe was still oblate (as also suggested by [1, 2, 3]). We also discuss the stability of our model to small perturbations around biaxiality and draw an analogy with cosmological perturbations. We conclude by presenting a separate, bouncing solution, which generalises the known bouncing solution in closed FRW universes.

PACS numbers: 98.80.Bp, 98.80.Cq, 98.80.Jk, 04.20.Dw, 04.20.Jb, 04.20.dc

Keywords: scalar fields, Bianchi models, big bang singularity, cosmology, exact solutions, Taub-NUT

^{*}Electronic address: p.dechant@mrao.cam.ac.uk

[†]Electronic address: a.n.lasenby@mrao.cam.ac.uk

[‡]Electronic address: mph@mrao.cam.ac.uk

I. INTRODUCTION

At the core of most of theoretical cosmology lie the assumptions of homogeneity and isotropy. These were originally motivated by the cosmological principle and the mathematical tractability of the resulting FRW models. However, the observed universe is obviously neither homogeneous nor isotropic, so these symmetries can only ever be approximate. Thus the question arises as to which assumptions we can relax whilst maintaining analytical tractability. We choose here to consider more general, anisotropic cosmologies, whilst keeping the assumption of (large-scale) spatial homogeneity. The resulting class of cosmologies is collectively known as the Bianchi models.

Scalar fields are ubiquitous in theories of high energy physics. The Standard Model of particle physics postulates the scalar Higgs particle, and Superstring Theory and string-inspired models motivate a plethora of moduli fields from compactifications, dilatons, radions etc. Scalar fields are also of interest in cosmology, as they can drive periods of accelerated expansion of the universe in a relatively straightforward and plausible manner. Cosmological scalar fields could therefore account for the posited period of inflation and the apparent present period of Λ -domination.

It is therefore natural to consider the effects of a scalar field dominating the dynamics of a Bianchi model. However, the phenomenological success of FRW models suggests that we should only consider the Bianchi classes that allow FRW universes as special cases. This narrows the phenomenologically interesting Bianchi types down to I, V, VII_h and IX. From previous work [4, 5] we are particularly interested in closed models, which are still consistent with observations [6]. The only closed Bianchi type that also allows for FRW subclasses is Bianchi IX, so we shall consider the dynamics of a scalar field in a Bianchi IX model [7, 8, 9]. Bianchi IX models are known to have very complicated dynamics, exhibiting oscillatory singularities and chaos (mix-master) [10, 11, 12, 13, 14, 15, 16, 17]. In this light, it is even more intriguing that the biaxial model we will consider is so well-behaved.

It is interesting that our solution provides another example of a regular solution with axial symmetry; for others, see Pitrou et al [1, 2] and Senovilla and collaborators [18, 19, 20, 21]. In the different context of inhomogeneous but axially symmetric cosmologies, [18, 19, 20, 21] also consider the important concept of geodesic completeness of a spacetime. Completeness is a criterion for the physical significance of a solution that is more stringent than mere geometric regularity, which we will also need to address later.

Often inflation is invoked to justify the assumptions of (acausal) homogeneity and isotropy. However, this then raises the question of how sensitive inflation itself is to the rather unnatural initial conditions of a homogeneous initial state. For these considerations, the interested reader may refer to, for instance, [22]. Here, however, we consider a Bianchi geometry as our starting assumption, without invoking inflation in order to justify it. For recent related literature concerning the case where a vector field is present to drive a phase of anisotropic inflation, see for example [23, 24].

This paper is organised as follows. We begin with a brief introduction to Bianchi models in Section II. In Section III we construct a generic Bianchi IX model dominated by scalar field matter and then specialise to the biaxial case in Section IV. (An alternative form of the Einstein field equations for this system, using the 3 + 1 covariant approach, is presented in the appendix.) We demonstrate scaling behaviour of solutions, and present a particular series solution, in which one radius goes to zero at the Big Bang (pancaking). We also consider geodesics through the Big Bang. We then present a realistic cosmology based on our model in Section V and, in Section VI, the stability of such a model about biaxiality. We finally present a separate, bouncing solution in Section VII, before we conclude in Section VIII.

II. BIANCHI UNIVERSES

Bianchi universes are spatially homogeneous and therefore have a 3-dimensional group of isometries G_3 acting simply transitively on spacelike hypersurfaces. The standard classification follows Bianchi's (1897) classification of 3-parameter Lie groups [25].

We adopt the metric convention $(+ - - -)$. Roman letters $a, b, c \dots$ from the beginning of the alphabet denote Lie algebra indices. Greek letters $\mu, \nu, \sigma \dots$ label spacetime indices, whereas Roman letters $i, j, k \dots$ from the middle of the alphabet label purely spatial ones.

The isometry group of a manifold is isomorphic to some Lie group G and the Killing vectors obey $[\xi_\mu, \xi_\nu] = C_{\mu\nu}^\sigma \xi_\sigma$ where the $C_{\mu\nu}^\sigma$ are the structure constants of G , so Lie groups can be used to describe symmetries, in particular, isometries.

When studying symmetries, an invariant basis is often useful. This is a set of vector fields X_μ each of which is invariant under G , i.e. has vanishing Lie derivative with respect to all the Killing vectors such that

$$[\xi_\mu, X_\nu] = 0. \tag{1}$$

Such a basis can be constructed simply by imposing this relation at a point for some chosen set of independent vector fields and using the Killing vectors to drag them out across the manifold. The integrability condition for this set of first-order differential equations amounts to demanding that the $C_{\mu\nu}^\sigma$ be the structure constants of some group. The invariant vector fields in fact satisfy

$$[X_\mu, X_\nu] = -C_{\mu\nu}^\sigma X_\sigma. \quad (2)$$

Denoting the duals of the X_μ by ω^μ , the corresponding curl relations for the dual basis are

$$d\omega^\mu = \frac{1}{2} C_{\sigma\tau}^\mu \omega^\sigma \wedge \omega^\tau. \quad (3)$$

Because the X_μ are invariant vectors, the metric can now be expressed as

$$ds^2 = g_{\mu\nu} \omega^\mu \omega^\nu, \quad (4)$$

for some $g_{\mu\nu}$.

Bianchi models can be constructed in various different ways. They are based on properties of a tetrad $\{\mathbf{e}_i\}$ that commutes with the basis of Killing vectors $\{\xi_j\}$ which generate the symmetry group

$$[\mathbf{e}_i, \xi_j] = 0. \quad (5)$$

Here we have made use of the fact that for homogeneous cosmologies there exists a preferred foliation of the 4-dimensional spacetime into a product spacetime with a timelike Killing vector and a 3-dimensional group of isometries G_3 acting simply transitively on spacelike hypersurfaces such that the timelike Killing vector commutes with the spacelike Killing vectors. Therefore we change from spacetime indices to spatial indices. We also adopt the comoving gauge whereby the timelike basis vector is taken as parallel to the unit normal to the surfaces of homogeneity. In general, the structure constants of the symmetry groups of these different surfaces of constant time are time-dependent [15, 26, 27]. However, from (5), it follows that between homogeneous slices, the structure constants are preserved up to a time-dependent linear transformation. One is free to shift the time dependence between the structure constants and the metric components by adjusting the time evolution of the tetrad. We choose to put all the time variation in the spatial metric components such that

$$ds^2 = dt^2 - \gamma_{kl}(t)(e_i^k(x)dx^i)(e_j^l(x)dx^j), \quad (6)$$

where $e_i^k(x)$ are the one-forms inverse to the spatial tetrad which have the same structure constants C_{ij}^k as the isometry group and commute with the timelike unit normal \mathbf{e}_0 to the surfaces of homogeneity: $\mathbf{e}_0 = \partial_t$ and $\mathbf{e}_i = e_i^j \partial_j$, such that $[\mathbf{e}_i, \mathbf{e}_j] = C_{ij}^k \mathbf{e}_k$ and $[\mathbf{e}_0, \mathbf{e}_i] = 0$. This is the approach we will adopt for constructing the metric later, as the Einstein field equations become ordinary differential equations in the metric components $\gamma_{ij}(t)$. (Other approaches are based on the automorphism group of the symmetry group [28, 29] or put the time-dependence in the commutation functions of the basis vectors [30].)

We will now briefly review the Bianchi classification of G_3 group types. The spatial part of the structure constants C_{ij}^k can be decomposed into irreducible parts as follows

$$C_{ij}^k = \varepsilon_{ijl} n^{lk} + a_i \delta_j^k - a_j \delta_i^k \quad (7)$$

for n^{ij} symmetric. The Jacobi identities can then be rewritten as

$$n^{ij} a_j = 0. \quad (8)$$

Without loss of generality we can choose the tetrad so as to diagonalise $n_{ij} = \text{diag}(n_1, n_2, n_3)$ and to set $a^i = (a, 0, 0)$ which reduces the Jacobi identities to $n_1 a = 0$. This then allows one to classify the possible Lie groups. We can define two broad classes of structure constants according to whether $a = 0$ (Class A) or not (Class B). See Table I for more details concerning the individual Bianchi types specified by the different options for the n^{ij} matrix entries.

If one were to put the time dependence in the structure constants instead, one would of course have to show that the classification type must be preserved by the evolution equations for $n(t)$ and $a(t)$. It turns out that it is a generic property of the Einstein field equations that they preserve symmetries in initial data within its Cauchy development, so that the classification is in fact independent of which approach one chooses [31].

III. TRIAXIAL BIANCHI IX MODEL

We now consider Einstein-Hilbert gravity in a generic Bianchi IX model with a minimally coupled scalar field. For generality we also include a cosmological constant term. We therefore start with the action

$$S = \int d^4x \sqrt{-g} \left[\frac{1}{2\kappa} (R + 2\Lambda) - \frac{1}{2} \nabla_\mu \phi \nabla^\mu \phi + V(\phi) \right], \quad (9)$$

| Class | Type | n_1 | n_2 | n_3 | a | |
|-------|------------------|-------|-------|-------|----------|---------------------------|
| A | I | 0 | 0 | 0 | 0 | |
| | II | + | 0 | 0 | 0 | |
| | VI ₀ | 0 | + | - | 0 | |
| | VII ₀ | 0 | + | + | 0 | |
| | VIII | - | + | + | 0 | |
| | IX | + | + | + | 0 | |
| B | V | 0 | 0 | 0 | + | |
| | IV | 0 | 0 | + | + | |
| | VI _h | 0 | + | - | + | $h \equiv a^2/n_2n_3 < 0$ |
| | III | 0 | + | - | n_2n_3 | |
| | VII _h | 0 | + | + | + | $h \equiv a^2/n_2n_3 > 0$ |

TABLE I: Bianchi model classification. Those containing FRW models as special cases are: Bianchi IX (closed); Bianchi I and Bianchi VII₀ (flat); Bianchi V and Bianchi VII_h (open).

where R is the Ricci scalar, ϕ the scalar field and $V(\phi)$ its potential, which we will for simplicity assume to be that of a simple massive scalar field, $V(\phi) = \frac{1}{2}m^2\phi^2$. Variation of the action with respect to the scalar field ϕ yields conservation of energy-momentum

$$\nabla_\mu T^{\mu\nu} = 0, \quad (10)$$

for the usual scalar field energy-momentum tensor

$$T_{\mu\nu} = \phi_{;\mu}\phi_{;\nu} - g_{\mu\nu} \left(\frac{1}{2}\phi^{;\rho}\phi_{;\rho} - V(\phi) \right). \quad (11)$$

Variation with respect to the metric yields the Einstein field equations

$$G_{\mu\nu} = \kappa T_{\mu\nu} + \Lambda g_{\mu\nu}. \quad (12)$$

We are working in Planck units where $c = \hbar = 1$ and we will set $\kappa = 8\pi G$ to unity eventually.

We choose to express the Bianchi IX metric in the form

$$ds^2 = dt^2 - \frac{1}{4}\gamma_{ij}(t)\omega^i\omega^j \quad (13)$$

for $\gamma_j(t) = \text{diag}(R_1^2(t), R_2^2(t), R_3^2(t))$ and invariant 1-forms ω^i given by

$$\begin{aligned}\omega^1 &\equiv dx + \sin y dz, \\ \omega^2 &\equiv \cos x dy - \sin x \cos y dz, \\ \omega^3 &\equiv \sin x dy + \cos x \cos y dz,\end{aligned}\tag{14}$$

with corresponding Killing vectors (these just correspond to the rotations of the 3-sphere, i.e. the Clifford translations)

$$\begin{aligned}\xi_1 &\equiv \sec y \cos z \partial_x + \sin z \partial_y - \tan y \cos z \partial_z, \\ \xi_2 &\equiv -\sec y \sin z \partial_x + \cos z \partial_y + \tan y \sin z \partial_z, \\ \xi_3 &\equiv \partial_z,\end{aligned}\tag{15}$$

and invariant basis

$$\begin{aligned}X_1 &\equiv \partial_x, \\ X_2 &\equiv \sin x \tan y \partial_x + \cos x \partial_y - \sin x \sec y \partial_z, \\ X_3 &\equiv -\cos x \tan y \partial_x + \sin x \partial_y + \cos x \sec y \partial_z\end{aligned}\tag{16}$$

taken from [32]. (We will consider an alternative set of Killing vectors derived within the Conformal Geometric Algebra framework [33, 34] related more obviously to an (x, y, z) coordinate system in a future work.)

Using the above expressions for the generating one-forms and expanding out we get the following non-zero metric components for a triaxial Bianchi IX universe (where we have dropped the explicit time dependence of the scale factors $R_i(t)$ for the sake of brevity):

$$\begin{aligned}g_{tt} &= 1, \\ g_{xx} &= -\frac{1}{4}R_1^2, \\ g_{yy} &= -\frac{1}{4}(R_2^2 \cos^2 x + R_3^2 \sin^2 x), \\ g_{zz} &= -\frac{1}{4}[R_1^2 \sin^2 y + (R_2^2 \sin^2 x + R_3^2 \cos^2 x) \cos^2 y], \\ g_{xz} &= -\frac{1}{4}R_1^2 \sin y, \\ g_{yz} &= -\frac{1}{4}(R_3^2 - R_2^2) \sin x \cos x \cos y.\end{aligned}\tag{17}$$

Introducing the usual definitions for the Hubble parameters

$$H_i(t) \equiv \frac{\dot{R}_i}{R_i}\tag{18}$$

for the three different directions, we find that for the above metric the conservation of energy-momentum (10) corresponds to the Klein-Gordon-type equation

$$m^2\phi + (H_1 + H_2 + H_3)\dot{\phi} + \ddot{\phi} = 0. \quad (19)$$

The ti -components of the Einstein field equations (for spatial index i) give three dynamical equations for the Hubble parameters H_i , the first of which reads

$$2\dot{H}_1 = H_2H_3 - 2H_1^2 - H_1H_3 - H_1H_2 + \Lambda - \kappa p - \frac{5R_1^2}{R_2^2R_3^2} + \frac{3R_2^2}{R_3^2R_1^2} + \frac{3R_3^2}{R_1^2R_2^2} - \frac{6}{R_1^2} + \frac{2}{R_2^2} + \frac{2}{R_3^2}, \quad (20)$$

and the other two equations are obtained simply by swapping indices $1 \leftrightarrow 2$ and $1 \leftrightarrow 3$. The tt -component of the Einstein field equations yields one Friedmann-type constraint equation

$$-H_1H_2 - H_2H_3 - H_1H_3 + \Lambda + \kappa\rho + \frac{R_1^2}{R_3^2R_2^2} + \frac{R_2^2}{R_3^2R_1^2} + \frac{R_3^2}{R_1^2R_2^2} - \frac{2}{R_1^2} - \frac{2}{R_2^2} - \frac{2}{R_3^2} = 0, \quad (21)$$

where $\rho = \frac{1}{2}\dot{\phi}^2 + V(\phi)$ and $p = \frac{1}{2}\dot{\phi}^2 - V(\phi)$ are the energy density and pressure of the scalar field matter respectively. Note that there are no spatial gradients of ϕ in the expressions for ρ and p , by spatial homogeneity. The case of vanishing potential corresponds to a stiff fluid, $p = \rho$, which has been investigated in [35, 36], amongst others.

For different applications, it might be useful to recast these equations in terms of the averaged scale factor, i.e. the volume expansion,

$$R \equiv (R_1R_2R_3)^{\frac{1}{3}}, \quad (22)$$

its associated Hubble factor,

$$3H \equiv H_1 + H_2 + H_3, \quad (23)$$

and the shear σ_{ij} . For example, this would be useful for separating the contributions from the curvature and the shear. We display this form of the Einstein field equations in the appendix. In the case of the biaxial Bianchi IX model that we will consider shortly, however, we believe the parametrisation in terms of the different radii is clearer. When considering the cosmology at late times, however, we will find that our model has isotropised sufficiently such that we can describe our model by an effective FRW-model with a scale factor given by the volume expansion of the Bianchi model.

It has been known for a long time that the Bianchi IX model (or indeed any Bianchi model for which $C_{ij}^j = 0$) is geodesically incomplete and exhibits a curvature singularity for perfect fluid matter (see, e.g. [37]). The singularity occurs precisely when the volume of an invariant hypersurface goes to zero. The perfect fluid energy density can be shown to diverge as $\rho_{fl} \sim \frac{1}{t}$ and the curvature invariants are singular as well, as $t \rightarrow 0$. However, it is the oscillatory character of the singularity that makes perfect fluid matter in a Bianchi IX universe model unsatisfactory as a cosmological model: the Big Bang is an essential singularity. Oscillations in the ratios of the different scale factors in $\ln(t)$ effectively show that there is an infinite history upon approaching the Big Bang, making it impossible to trace back to it. Conversely, coming out of an essential singularity to reach the observed universe is ill-defined for the same reasons. This also holds, in particular, for the biaxial case by virtue of the general theorem. We will see below that for a biaxial Bianchi IX model with scalar field matter, however, the picture will be qualitatively different.

Scalar field matter is still unsatisfactory in the full triaxial Bianchi IX model, however, since it exhibits the same behaviour outlined above. As we show below, it is only when we impose axial symmetry, that a solution is possible in which all physical quantities such as energy density and curvature invariants remain finite at the Big Bang, and the universe extends smoothly across what is no longer an essential singularity into a well-behaved pre-Big Bang phase (though parity-inverted!). This then raises the question as to whether the axially symmetric case is stable to small perturbations in biaxiality, which we will address in Section VI.

IV. BIAXIAL BIANCHI IX MODEL

We therefore now specialise to the case where two of the axes are equal, $R_2(t) = R_3(t)$, which leads to the simplified metric (again with the t -dependence of the scale factors suppressed)

$$g_{\mu\nu} \equiv \begin{pmatrix} 1 & 0 & 0 & 0 \\ 0 & -\frac{1}{4}R_1^2 & 0 & -\frac{1}{4}R_1^2 \sin y \\ 0 & 0 & -\frac{1}{4}R_2^2 & 0 \\ 0 & -\frac{1}{4}R_1^2 \sin y & 0 & -\frac{1}{4}(R_1^2 \sin^2 y + R_2^2 \cos^2 y) \end{pmatrix}. \quad (24)$$

Now there are only two dynamical equations, for the two non-degenerate Hubble parameters, and one Friedmann constraint. The first dynamical equation is

$$2\dot{H}_2 + 3H_2^2 + \kappa p - \Lambda = \frac{1}{R_2^2} \left(3\frac{R_1^2}{R_2^2} - 4 \right) \quad (25)$$

and the other reduces to

$$2\dot{H}_1 + 2H_1^2 - H_2^2 + 2H_1H_2 + \kappa\rho - \Lambda = -\frac{1}{R_2^2} \left(5\frac{R_1^2}{R_2^2} - 4 \right). \quad (26)$$

In the isotropic limit, these equations reduce to appropriate combinations of the usual Friedmann and acceleration equations, as required. The Einstein field equations further yield the Friedmann constraint

$$H_2^2 + 2H_1H_2 - \kappa\rho - \Lambda = \frac{1}{R_2^2} \left(\frac{R_1^2}{R_2^2} - 4 \right). \quad (27)$$

This is straightforwardly seen to reduce to the standard Friedmann equation as $R_1 \rightarrow R_2 = R_3$. The equations of motion for the matter content follow straightforwardly from energy-momentum conservation as above. In fact they are easily deduced from the triaxial case and read

$$m^2\phi + (H_1 + 2H_2)\dot{\phi} + \ddot{\phi} = 0. \quad (28)$$

We prefer the viewpoint from which the equations (25)-(26) are dynamical equations for the Hubble parameters and regard the scale factors R_i as derived quantities, but these equations are obviously equivalent to second order equations in terms of the radii.

The simplicity of these equations suggests that a relatively simple solution should be possible. We are particularly interested here in solutions with definite parity, and defer discussion of solutions with indefinite parity to a future work. We show below that both odd-parity and even-parity series expansions exist around the ‘Big Bang’, which are therefore valid starting points for numerical integration, but first we briefly discuss the generation of a family of solutions from a given solution by scaling.

A. Families of solutions related by scaling

Given a solution to the equations (25)-(28), a family of solutions is generated by scaling with a constant σ and defining

$$\bar{R}_i(t) = \frac{1}{\sigma}R_i(\sigma t), \quad \bar{H}_i(t) = \sigma H_i(\sigma t), \quad \bar{\phi}(t) = \phi(\sigma t), \quad \bar{m} = \sigma m, \quad \bar{\Lambda} = \sigma^2\Lambda. \quad (29)$$

(This scaling is in fact analogous to the one found previously in [4].) This scaling property is valuable for numerical work, as a range of situations can be covered by a single numerical integration. Furthermore, many physically interesting quantities turn out to be invariant under changes in scale. This scaling property does not, however, survive quantisation, so one would have to be careful when considering vacuum fluctuations.

B. Odd-parity series expansion around the ‘Big Bang’

It is well known [15, 37] that pancake singularities (which we will identify with the ‘Big Bang’, and choose to happen at time $t = 0$), where one radius goes to zero and the other two remain finite as $t \rightarrow 0$, can occur in Bianchi models. This is already in some sense an improvement over the FRW case, where the singularity is pointlike. However, pancake singularities are known to occur in Bianchi I (as well as cigar singularities), whereas Bianchi IX is commonly thought generically to exhibit oscillatory singularities. We will now show that, with scalar field matter, the pancake singularity in the Bianchi IX model is not in fact a curvature singularity at all, because all physical quantities remain finite as $t \rightarrow 0$ and extend smoothly into a parity-inverted universe for $t < 0$.

We assume that it is the non-degenerate radius R_1 that tends to zero as $t \rightarrow 0$. Close to the Big Bang, the linear term becomes dominant for $R_1(t)$, whereas the other radii $R_2(t) = R_3(t)$ tend to a non-zero constant, as does the scalar field $\phi(t)$. Indeed, for a series solution ansatz in which we assume oddness for R_1 and evenness for the other functions, i.e.

$$\begin{aligned} R_1(t) &= t (a_0 + a_2 t^2 + a_4 t^4 + \dots) \\ R_2(t) = R_3(t) &= b_0 + b_2 t^2 + b_4 t^4 + \dots, \\ \phi(t) &= f_0 + f_2 t^2 + f_4 t^4 + \dots \end{aligned} \tag{30}$$

then the three dynamical equations (25), (26) and (28) allow us to fix the three series term-by-term, given the initial values $a_0 = \dot{R}_1(0)$, $b_0 = R_2(0)$ and $f_0 = \phi(0)$. The fact that this also satisfies the Friedmann energy constraint (27) then proves that this odd-parity series solution is a valid expansion around the Big Bang, which we can use as a starting point for numerical integration.

Intriguingly, it turns out that the spacetime is non-singular insofar as the Riemann tensor is well-behaved at the Big Bang and so are all curvature invariants. In fact only three components of the Riemann tensor are non-zero at $t = 0$:

$$R_{tyty} = \frac{1}{16} \kappa m^2 f_0^2 b_0^2 + \frac{1}{8} \Lambda b_0^2 - \frac{1}{2}, \quad R_{tztz} = R_{tyty} \cos^2 y, \quad R_{yzyz} = -\frac{1}{4} b_0^2 \cos^2 y. \tag{31}$$

The fact that there is no curvature singularity means that these series solutions can be continued through to negative values of t . That is, $R_2 = R_3$ and ϕ are even for $t < 0$, whereas R_1 is odd i.e. negative for $t < 0$. This amounts to a parity inversion at the Big Bang. Instantaneously, as the hypersurface volume goes to zero at the Big Bang, the spatial hypersurface is 2-dimensional.

The fact that the universe can be momentarily ‘dimensionally reduced’ is interesting. Nonetheless, even though the hypersurface volume goes to zero instantaneously, information about the evolution is encoded in the derivatives. If one adopts the string-inspired viewpoint [38, 39, 40] that the universe could be described by a 3-brane, the instantaneous conversion of 3-branes into 2-branes seems problematic in type IIA and IIB String theory, but could be interesting from a type IIA/IIB String theory duality or AdS/CFT point of view. From a more conservative perspective, this process resembles Taub-NUT space [37, 39], which is a biaxial Bianchi IX vacuum solution that can be represented as a disc that evolves into an ellipsoid and back into a disc. It therefore also shows the same feature of dimensional reduction as our model, and moreover also does not have a geometric singularity during this collapse. In particular, it is thought to evolve from timelike open sections in a NUT region, via lightlike sections (called Misner bridges), to spacelike closed sections in the Taub region, back into timelike open sections in the other NUT region. This open-to-closed-to-open transition is not mathematically singular, but it is incomplete, as geodesics spiral infinitely many times around the topologically closed spatial dimension as they approach the boundary [41, 42]. This type of singularity is called ‘quasiregular’ in the Ellis and Schmidt classification [43] (these include the well-known ‘conical’ singularities [44]), as opposed to a (scalar or non-scalar) curvature singularity. For completeness, a possible parametrisation for the Taub-NUT metric is

$$ds^2 = 2dt\omega^1 - \frac{1}{4}R_1^2(\omega^1)^2 - \frac{1}{4}R_2^2[(\omega^2)^2 + (\omega^3)^2] \quad (32)$$

as compared with

$$ds^2 = dt^2 - \frac{1}{4}R_1^2(\omega^1)^2 - \frac{1}{4}R_2^2[(\omega^2)^2 + (\omega^3)^2] \quad (33)$$

in our model. The interested reader may refer to [37], for example, for a discussion of Taub-NUT.

It is worth noting that in deriving the above series solution, one can instead start with a general Taylor series expansion in the full triaxial case. Expanding around the Big Bang rather than any other point amounts to demanding that the constant term in the Taylor expansion for R_1 be zero (in fact, this could be any radius, as R_1 is not special in the triaxial case), whereas everything else is in principle undetermined. Imposing the dynamical equations, however, forces the two non-zero radii to be the same term-by-term for the expansion to be valid, i.e. a Big Bang-like expansion only works for the axisymmetric model; there is an essential singularity unless we consider the special, biaxial case. The validity of the equations of motion further implies the above mentioned even form for $R_2 = R_3$ and ϕ , and odd behaviour for R_1 .

Since the existence of the above series expansion around the Big Bang demonstrates that an axisymmetric pancake singularity is a valid starting point for numerical integration, we therefore solved the biaxial equations numerically subject to the appropriate boundary conditions. We found good agreement with the series solutions within the range of their validity. The large parameter space of this model admits both viable (in the sense of compatible with present observations) and unrealistic (in the sense of incompatible with present observations) cosmologies. We defer seeking realistic model parameters and displaying the numerical results until Section V and instead concentrate next on addressing the issue of geodesic completeness.

C. Behaviour of geodesics

As we have shown, our model has no curvature singularity at the Big Bang, at which all physical quantities remain finite. Thus, at the level of the evolution equations, the model is well-behaved. We now consider the question of geodesic completeness of our model to determine whether it possesses a non-curvature singularity at $t = 0$.

The geodesic equations are most easily obtained using the Lagrangian formalism, in which

$$L = \frac{1}{4} g_{\mu\nu} \dot{x}^\mu \dot{x}^\nu \quad (34)$$

is varied with respect to the coordinates $[x^\mu] = (t, x, y, z)$; here a dot denotes a derivative with respect to some affine parameter λ and the factor $\frac{1}{4}$ is included for later convenience. Inserting the biaxial metric (24) into L yields

$$L = 4\dot{t}^2 - R_1^2 \dot{x}^2 - 2R_1^2 \sin y \dot{x} \dot{z} - R_2^2 \dot{y}^2 - (R_1^2 \sin^2 y + R_2^2 \cos^2 y) \dot{z}^2. \quad (35)$$

Since L is independent of the x - and z -coordinates, the corresponding Euler–Lagrange equations yield two conserved quantities K_x and K_z according to the relations

$$-2R_1^2 (\dot{x} + \sin y \dot{z}) \equiv K_x, \quad (36)$$

$$-2 [R_1^2 \sin y (\dot{x} + \sin y \dot{z}) + R_2^2 \cos^2 y - \dot{z}] \equiv K_z, \quad (37)$$

which may be solved for \dot{x} and \dot{z} to yield

$$\dot{x} = \frac{K_z R_1^2 \sin y - K_x (R_1^2 \sin^2 y + R_2^2 \cos^2 y)}{2R_1^2 R_2^2 \cos^2 y}, \quad (38)$$

$$\dot{z} = \frac{K_x \sin y - K_z}{2R_2^2 \cos^2 y}. \quad (39)$$

Substituting these expressions back into the Lagrangian, the Euler–Lagrange equation for y then reads

$$4R_2^3 \cos^3 y \left(R_2 \ddot{y} + 2 \frac{\partial R_2}{\partial t} \dot{y} \right) = (K_x^2 + K_z^2) \sin y - 2K_x K_z + K_x K_z \cos^2 y. \quad (40)$$

Let us first consider null geodesics for which $g_{\mu\nu} \dot{x}^\mu \dot{x}^\nu = 0 = L/4$. To begin with, we wish only to show that some geodesics extend smoothly through the Big Bang, and therefore we can choose a convenient form. Inspection of equations (38) and (39) shows that we cannot set either of \dot{x} and \dot{z} alone to zero by choosing suitable constants, but we can consider the case where both vanish (this requires the choice $K_x = K_z = 0$ and essentially corresponds to motion in the y -direction). In this case the Euler–Lagrange equation for y simplifies to $d(R_2^2 \dot{y})/d\lambda = 0$ which can be immediately integrated to yield

$$R_2^2 \dot{y} = K_y, \quad (41)$$

where K_y is another constant of the motion. The constraint that the geodesic is null now reads $4\dot{t}^2 - R_2^2 \dot{y}^2 = 0$, which gives

$$\frac{dy}{dt} = \frac{\dot{y}}{\dot{t}} = \pm \frac{2}{R_2}. \quad (42)$$

This is reminiscent of the Friedmann case, but one must now bear in mind that in our model R_2 is finite and non-zero at the Big Bang in contrast to the scale factor in an FRW model. Thus, there is no longer a difficulty in integrating through the Big Bang; rather, it is trivial. Indeed, looking at the Euler–Lagrange equation for y directly in this case, one has

$$R_2 \ddot{y} + 2 \frac{\partial R_2}{\partial t} \dot{y} = 0, \quad (43)$$

which amounts to $\ddot{y} = 0$ near the Big Bang where R_2 has a minimum, also suggesting that such a light ray goes straight through the Big Bang. Thus photon motion in y is effectively undisturbed by the pancaking.

Let us now consider a photon moving in the x -direction. It is easiest to see from (40) that if a photon starts at $y = 0$ it will stay there. Hence for $K_z \equiv 0$ and $y = 0$, the results (38), (39) and (40) yield $\dot{z} = 0$, $\dot{y} = 0$ and

$$\dot{x} = -\frac{K_x}{2R_1^2}. \quad (44)$$

In this case, the constraint that the geodesic is null yields $4\dot{t}^2 = R_1^2 \dot{x}^2$. Hence, close to $t = 0$, where R_1 is approximately linear in t , once has

$$\frac{dx}{dt} = \frac{\dot{x}}{\dot{t}} = \pm \frac{2}{R_1} \propto \pm \frac{1}{t}. \quad (45)$$

Integrating we obtain

$$x(t) = c_1 \ln(-t) + c_2 \quad \text{or} \quad x(t) = c_3 \ln(t) + c_4, \quad (46)$$

for some constants c_i , $i = 1 \dots 4$, which shows that at $t < 0$ we must have the former solution and at $t > 0$ the latter.

Let us illustrate these solutions by considering the specific case of a photon travelling in the positive x -direction as time increases, i.e. $\frac{dx}{dt} > 0$. For $t < 0$ we have $\frac{dx}{dt} = \frac{c_1}{t}$ and for this to be positive for negative t we must have $c_1 < 0$. This also yields $R_1 \approx -\frac{2}{c_1}t$ from (45) which is negative for $t < 0$ as expected. For $t > 0$ (46) yields $\frac{dx}{dt} = \frac{c_3}{t} > 0$ so $c_3 > 0$ and $R_1 \approx \frac{2}{c_3}t$. So it seems that the photon x -coordinate goes to $+\infty$ as $t \rightarrow 0$ from below, reappearing just after $t = 0$ at $x = -\infty$. This is less problematic than it seems: the spatial sections in Bianchi IX are topologically S^3 , so it is natural to think of the coordinates as angles that should be periodically identified. Furthermore, at $t = 0$ and therefore $R_1 = 0$, (6) yields vanishing proper distance between different values of x , which presumably means that this direction has shrunk to a point. Since our coordinates are angles, the result of the photon going to ∞ appears to signify that the geodesics are infinitely spiralling (which is reminiscent of Taub-NUT) around a closed spatial dimension as it is collapsing. The proper distance traversed and time taken both, however, become infinitesimally small, so the whole process might still be finite. Thus it is not clear that anything singular has in fact happened to the photon trajectory, despite appearances to the contrary; this will also be discussed further in a future work.

We will now consider massive particles, which travel along timelike geodesics. The only difference in this case is that one must now impose the timelike geodesic normalisation constraint $g_{\mu\nu}\dot{x}^\mu\dot{x}^\nu = 1 = L/4$. Let us again begin by considering a particle travelling in the y -direction. In this case, (41) still holds, but the normalisation constraint becomes $4\dot{t}^2 = 4 + R_1^2\dot{y}^2$. This yields

$$\frac{dy}{dt} = \pm \frac{2K_y}{\sqrt{4R_1^2 + K_y^2}}. \quad (47)$$

At $t = 0$, the right-hand side is still constant to first-order, mirroring the massless case, so massive particles motion in the y -direction is also essentially unaffected by the pancaking.

Finally, we consider motion of a massive particle along the x -direction. Again (44) holds, but the normalisation constraint is now $4\dot{t}^2 = 4 + R_1^2\dot{x}^2$, which yields

$$\frac{dx}{dt} = \frac{\dot{x}}{\dot{t}} = \mp \frac{2K_x}{R_1\sqrt{16R_1^2 + K_x^2}}. \quad (48)$$

Since $R_1 \approx Ct$ near $t = 0$, for a constant C , on integrating we obtain

$$x(t) = \frac{2}{C} \ln \left[\pm \frac{t}{2K_x \left(K_x + \sqrt{K_x^2 + 16C^2 t^2} \right)} \right], \quad (49)$$

In this regime the denominator in the logarithm is approximately constant so massive particles will display qualitatively precisely the same behaviour as photons as they approach and leave the point of pancaking.

Thus, in summary, we find that there are null and timelike geodesics that go smoothly through the Big Bang into a pre-Big Bang phase, but other such geodesics that spiral infinitely around a topologically closed spatial dimension. This issue does not seem to warrant too much concern for our model, owing to the periodic identification of these angular coordinates on the 3-spheres. This further supports our claim that this model is substantially better behaved than most conventional cosmological models. The issue of geodesic completeness will be further discussed in a future paper, but it is worth noting here that, even if the spacetime is incomplete, the singularity at the Big Bang can, at worst, be of quasiregular type [43] as occurs also in Taub-NUT [41, 42].

V. REALISTIC BIAxIAL BIANCHI IX COSMOLOGY

We now examine the viability of our model for providing a realistic cosmology. We begin by noting the argument of [4, 5], that there is a natural, geometrical boundary condition on the universe resulting from the need to match a Big Bang phase onto an asymptotic de Sitter phase within a particular type of conformal representation. Here a genuine cosmological constant Λ is being assumed, rather than a quintessence model. Using a conformal embedding and the symmetries of de Sitter space, a boundary condition is arrived at that the total elapsed conformal time should be equal to $\frac{\pi}{2}$. The condition is simply to demand that the future asymptotic de Sitter state be the future infinity surface of the conformal embedding. This amounts to imposing a boundary condition at temporal infinity, much like in (quantum) field theory. This singles out a particular flow line in $(\Omega_m, \Omega_\Lambda)$ space.

In the context of a closed FRW model, it is shown in [4, 5] that the conformal time constraint predicts within the correct range the degree of flatness of the universe, as well as the size of the cosmological constant. Moreover, the computed inflationary perturbations were shown to be consistent with WMAP data and could even account for the low- ℓ deficit. Extending this conformal time constraint to our Bianchi model, we find that this constraint can be satisfied by setting the

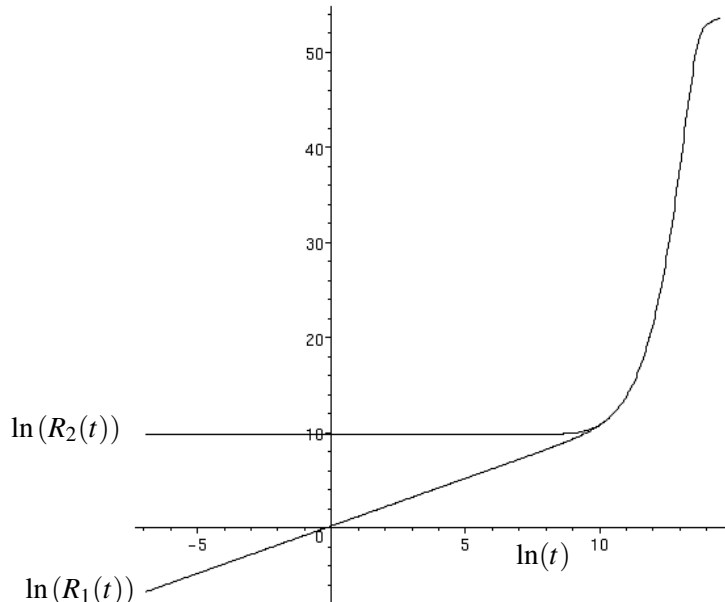


FIG. 1: Dynamics of the biaxial Bianchi IX model: evolution of the logarithm of the scale factors R_1 and R_2 in Planck lengths l_p versus log time (t in units of Planck time t_p).

free parameters in our model to $\kappa = 1$, $m = \frac{1}{64000}$, $a_0 = 1.2$, $b_0 = 18000$ and $f_0 = 13$. (These values are for κ set to 1, and are essentially a representative set, rather than having been fixed to get best agreement with current data.) These parameter values are all ‘natural’, but in order to fix the normalisation of the perturbation spectrum, the mass of the scalar field had to be rescaled and b_0 changes to a less natural value accordingly. This choice for the mass of the scalar field needs to be put in by hand for every model so does not constitute any unusual fine-tuning.

This model looks like the universe that we observe in the sense that it comes out of a Big Bang-like state, followed by an inflationary phase and eventually reaches a state of steady expansion (see Figure 1). There it can feasibly be matched onto a model of radiation domination followed by matter domination to recover our standard cosmology. Note, however, that this Bianchi model is interesting irrespective of our arriving at the particular parameter values above by using the conformal time condition.

As mentioned earlier, the model exhibits no curvature singularity, with all physical quantities remaining finite through the Big Bang. The fact that the vanishing radius is odd in time results in parity inversion as we go through the Big Bang. The property that the energy density remains finite is contrary to the most common scenarios (although it was previously known that a massive scalar field can lead to a non-singular bounce in the special case of a closed FRW universe; see

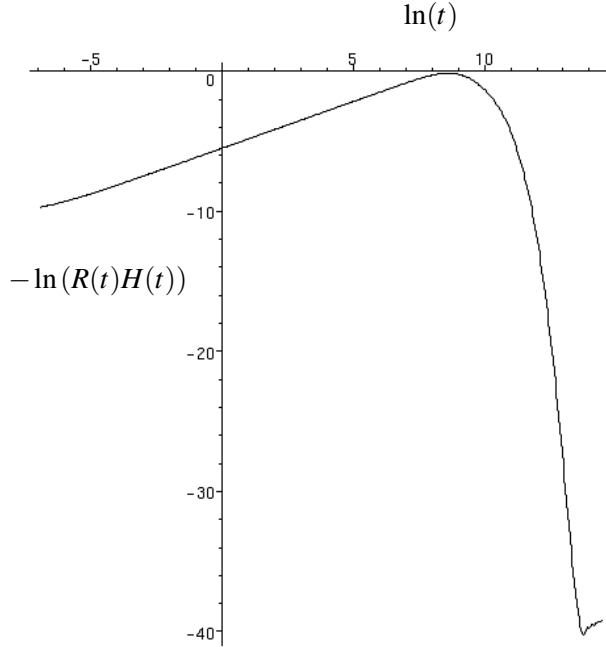


FIG. 2: Dynamics of the biaxial Bianchi IX model: evolution of the logarithm of the comoving Hubble radius versus log time. Note that the curvature radius $R(t) \equiv (R_1 R_2 R_3)^{\frac{1}{3}}$, with corresponding Hubble function $H(t) \equiv \frac{\dot{R}}{R}$ and associated Hubble radius H^{-1} . The parameters for the model are described in the text. During inflation, $1/(RH)$ decreases with time, corresponding to accelerated expansion. Thus this model leads to a period of inflation lasting approximately for the period $\ln t = 9 - 13.5$. All quantities are in Planck units.

[45] for more information on the history of such models).

Figure 1 demonstrates that the scale factor $R_1(t)$ approaches zero linearly as $t \rightarrow 0$, as expected from the series expansion in Section IV B. Note that this behaviour results in a slope of 1 in the log-log plot as $\ln t \rightarrow -\infty$. The other radii $R_2 = R_3$, as well as physical variables such as the scalar field and the scalar field energy density, tend to a constant at the Big Bang as shown in Figure 1, confirming our results from the series expansion. This shows that this model exhibits a pancake singularity. The relaxation of the assumption of isotropy makes a variety of singularities possible which generalise the pointlike FRW-singularity. For instance, pancake, barrel and cigar singularities are known to occur in Bianchi models [15, 37]. (In both barrel and cigar singularities, two scale factors tend to zero but the third increases without bound in cigar singularities, and approaches a constant in barrel singularities.) It is worth noting, however, that a pancake singularity is atypical for Bianchi IX models.

The evolution of the oblateness $R_2(t)/R_1(t)$ (see Figure 1), suggests that the evolution equations

favour the radii $R_2(t) = R_3(t)$ becoming similar to the radius $R_1(t)$, in agreement with the need to be tolerably close to an FRW cosmology at late times. (This ties in nicely with the fact demonstrated in Section VI that the biaxiality of our model, i.e. $R_2(t) = R_3(t)$, is also stable to sufficiently small perturbations of the type $R_3(t)/R_2(t) = 1 + \delta(t)$, thereby allowing an almost-FRW model in which all axes are similar.) Note, however, that Figure 1 demonstrates that the universe was significantly anisotropic until at least $\ln t \approx 10$. The scalar field seems to isotropise the universe and subsequently drive inflation. (For related literature on isotropisation, see [46, 47, 48, 49, 50].)

We can define an averaged scale factor by $R(t) \equiv (R_1 R_2 R_3)^{\frac{1}{3}}$, with which we can associate an averaged Hubble function $H(t) \equiv \dot{R}/R$, as usual, and thereby define a comoving Hubble radius $1/(RH)$. Figure 2 shows the evolution of the comoving Hubble radius $1/(RH)$ for our model. Inflation is a period of accelerated expansion, which results in the comoving Hubble radius $1/(RH)$ decreasing with time. From the plot we can infer that for our model a period of inflation does occur and lasts approximately from $\ln t \approx 9$ to $\ln t \approx 13.5$. During this inflationary period $\ln(R)$ increases from about 10 to 55 (c.f. Figure 1), corresponding to roughly 45 e-folds of inflation.

In order to produce the fluctuation spectrum observed in our own universe, it is thought that the present Hubble horizon must have been inflated by at least about 40-50 e-folds, that is, 40-50 e-folds between the time where the present Hubble scale exited the horizon and the end of inflation [51, 52]. This minimal number of e-folds would lead to a universe that departs from spatial flatness by an amount that is just visible today [53]. If more time was spent on the inflationary attractor, the universe would be driven closer to flatness and might in fact become indistinguishably close to spatially flat.

Since our model produces around 45 e-folds of inflation, for agreement with observations, we would therefore require that the present horizon scale leave the Hubble horizon soon after the onset of inflation. This is in agreement with Uzan, Kirchner and Ellis' estimates [52] and, in particular, also leads to a visibly closed geometry (cf. Starobinsky [53]).

Figures 1 and 2 show that the phases of isotropisation and inflation might have overlapped in the time period $\ln t \approx 9 - 10$ such that structure on the largest scales could have been laid down whilst the universe was still significantly oblate. In particular, we have just argued that the present horizon scale should have crossed the horizon around that time. So imprints of oblateness might actually be experimentally accessible to us. Such considerations, including perturbation analysis, CMB imprints, etc. will be described in future work. Clearly, a proper analysis must generalise standard inflationary cosmological computations [51, 54] to anisotropic cosmologies [55]. In

particular, there are subtleties regarding the correct choice of vacuum (generalisation of the Bunch-Davies vacuum), the definition of the canonical variables (generalisation of the Mukhanov-Sasaki variables), the discreteness of the eigenmodes of the Laplacian on the 3-sphere (as mentioned above, we use a continuum approximation) as well as the definition of k^2 , which arises since the direction of the wavevector k_i starts to matter due to the anisotropy. Since inflation drives the spacetime closer to flatness, it might also be possible to approximate the spacetime by a Bianchi I model and quantise the perturbations in this approximation as an intermediate step. There has been recent progress in the cosmological perturbation theory of Bianchi I models, to which the interested reader may wish to refer [1, 2, 3]. Their results further show that the two gravitational wave polarisations do not necessarily have the same power spectra. The spectra also do not seem to reduce to the standard results in the limit of vanishing shear. At very early times, when the shear dominates over the curvature, the Bianchi IX model is also very close to a Bianchi I model – though not topologically, of course. Note also that since the issue of how geodesics propagate through the pancaking is as yet not completely resolved, we only consider perturbations ‘this side’ of the pancaking, rather than trying to track or match perturbations from both sides [45, 56, 57].

As a first approximation, however, one may consider the slight anisotropy during inflation as a perturbation to standard FRW results and neglect it to zeroth order. In this case, the definition of a comoving wavevector k becomes unambiguous. A detailed computation would ultimately have to validate this approach. In this approximation the power spectrum of the curvature perturbation is given by

$$\mathcal{P}_{\mathcal{R}}(k) = 8\pi \left(\frac{H^2}{2\pi\dot{\phi}} \right)^2, \quad (50)$$

and the spectrum of the tensor perturbation by

$$\mathcal{P}_{grav}(k) = \left(\frac{16H^2}{\pi} \right), \quad (51)$$

where the right hand sides of these equations are to be evaluated when the corresponding comoving wavenumber k crosses the horizon. From this we can also define the tensor-to-scalar ratio

$$r = \frac{\mathcal{P}_{grav}}{\mathcal{P}_{\mathcal{R}}}, \quad (52)$$

evaluated at some suitable low k . Note that there is a factor of 8π premultiplying the standard result in equation (50). This is a consequence of the use of different conventions: $G \equiv 1$ in the standard derivation, whereas here we have set $8\pi G = \kappa \equiv 1$.

Non-flat universe models, of which Bianchi IX is an example, are more complicated than their flat counterparts in many respects. However, they have the decided advantage of having another length scale available at any time: their associated curvature scale R . As set out below, this allows one to compare length scales at different times directly, rather than having to use relations from the inferred history of the universe, such as the epochs of matter and radiation domination and reheating, the details of which are not well known. Note that current experiments do indeed allow for curvature contributions to Ω at the per cent level, making such computations consistent with observations.

The comoving Hubble radius, and therefore the radius of the spatial sections, is related to the density parameter by

$$\Omega - 1 = \frac{1}{(RH)^2}. \quad (53)$$

The evolution of Ω for our model is shown in Figure 3. During inflation, Ω is driven to unity from above, whereas after inflation $\Omega = 1$ becomes a separatrix rather than an attractor, and Ω increases away from unity again. This provides a relationship linking time, the density parameter and the curvature radius (and thereby other length scales). We are particularly interested in when certain length scales cross the horizon. The first case of interest is when quantum fluctuations on different scales leave the horizon during inflation and thereby seed structure formation. Second, once inflation is completed, progressively larger scales then re-enter the horizon. The advantage of having the curvature scale available in non-flat geometries is that we can link the two times of horizon crossing for a particular length scale in a straightforward and exact manner.

Consider some physical size d_0 at the present time. (For wave modes in such a spherical universe, d_0 will actually be quantised in units of $2\pi R_0/(n^2 - 1)^{1/2}$, where n is an integer. Here we will use a continuum approximation, however.) Scales grow commensurately with the scale factor during the expansion of the universe, such that

$$\frac{d}{R} = \frac{d_0}{R_0}. \quad (54)$$

(Here, quantities without indices are evaluated at an arbitrary time, i.e. their dependence on time is left implicit, whereas the subscript 0 denotes quantities evaluated at the present epoch.) Moreover, the size of the Hubble radius relative to the radius of the spatial sections is also changing over the course of cosmic history, as given by (53). Suppose d_0 occupies some fraction x_0 of the current Hubble radius H_0^{-1}

$$x_0 = \frac{d_0}{H_0^{-1}}. \quad (55)$$

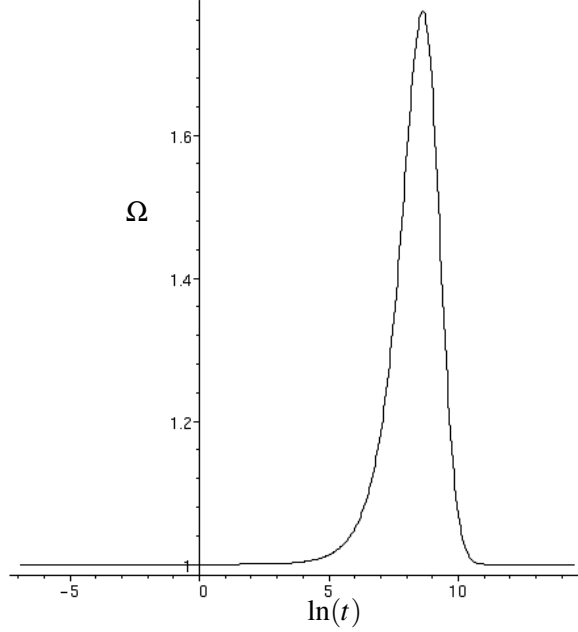


FIG. 3: Evolution of Ω . During inflation the total density is quickly driven to 1.

The ratio $x = dH$ will of course in general also change over time and obeys

$$x = dH = d_0 \frac{R}{R_0} H = x_0 \frac{RH}{R_0 H_0}. \quad (56)$$

Horizon crossing occurs when $x = 1$, i.e. the scale with a size d_0 at the present time left the horizon (i.e. Hubble length) at a time t given implicitly by

$$x_0 = \frac{R_0 H_0}{RH} = \frac{\sqrt{\Omega(t) - 1}}{\sqrt{\Omega_0 - 1}}. \quad (57)$$

where Ω_0 is the present value of the density parameter. As a simple example, the scale re-entering the horizon at the moment is, of course, the current Hubble horizon itself (for which $x_0 = 1$). Thus, from (57), the present Hubble radius left the horizon at a time t when $\Omega(t) = \Omega_0$ during inflation. So for comparison with observations, we are interested in scales that left the horizon after this epoch.

The WMAP 3-year results [6] quote 1.011 ± 0.012 . We shall therefore assume that $\Omega_0 \sim 1.01$. By the argument above, the time t at which the present Hubble radius left the horizon is given by the solution of $\Omega(t) = 1.01$ during inflation. This is, by virtue of equation (53), equivalent to $-\ln(RH) = -\ln 10 \approx -2.3$, which, referring back to Figure 2, occurs at $\ln(t) \approx 10.4$. Comparing with Figure 1, this corresponds to about one e-fold of inflation. This still leaves 44 e-foldings before the end of inflation, which is sufficient to provide a perturbation spectrum consistent with

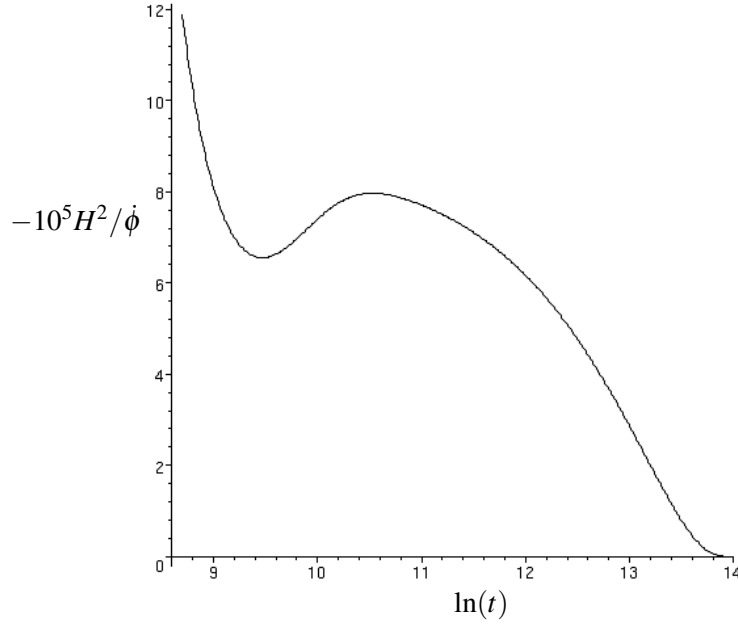


FIG. 4: Evolution of $H^2/\dot{\phi}$ during inflation. The function displayed is $-10^5 H^2/\dot{\phi}$ as a function of $\ln(t/t_p)$. This function determines the amplitude of the curvature perturbation.

experiments, in agreement with the estimates in [52]. Intriguingly, however, we can also extract the level of oblateness at that time from Figure 1 as $\sim 0.2\%$. This is to be regarded as significantly anisotropic, which means that structure on the largest scales would have been laid down when the universe was still oblate. This offers the exciting prospect of a possible experimental detection of imprints from such a time.

Having clarified how to evaluate the quantities given by (50) and (51), we note that the power spectrum of the curvature perturbation is controlled by the quantity $H^2/\dot{\phi}$, plotted in Figure 4. The curvature perturbation spectrum can now be computed from the joint knowledge of the evolution of Ω (Figure 3) and $H^2/\dot{\phi}$ (Figure 4). A physical wavenumber $k_{p,0}$ today is the inverse of the physical length scale d_0 and from (55) we find the physical wavenumber today that left the horizon at the time t from (57) is given by

$$\frac{1}{k_{p,0}} = \frac{x_0}{H_0}, \quad (58)$$

or, in comoving terms,

$$\frac{1}{k} = \frac{x_0}{R_0 H_0}. \quad (59)$$

Thus for a given comoving wavenumber k , equation (59) yields the corresponding value of x_0

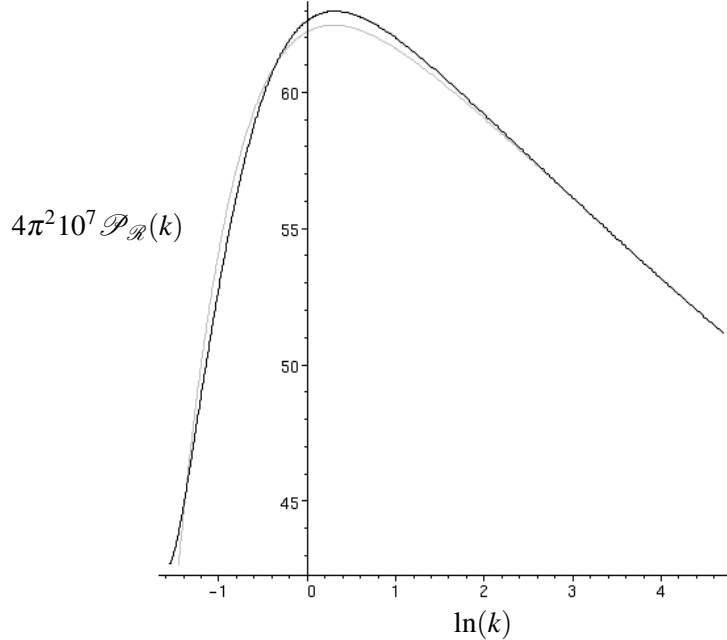


FIG. 5: The power spectrum of the curvature perturbation. $4\pi^2 10^7 \mathcal{P}_{\mathcal{R}}(k)$ is plotted as a function of $\ln(1/x_0) = \ln(k) + \text{constant}$. The grey line is a fit to the spectrum with an exponential cutoff proposed by Efstathiou. The parameters of the model and the cutoff are described in the text.

which is then substituted into (57) to obtain the time t when that scale left the horizon such that

$$\frac{1}{k} = x_0 \sqrt{\Omega_0 - 1} = \sqrt{\Omega(t) - 1}. \quad (60)$$

Figure 5 shows the curvature power spectrum as a function of $\ln(1/x_0) = \ln(k) + \text{constant}$ ($= \ln(k_{p,0}) + \text{constant}$). We again stress that, firstly, due to the isotropisation we are using an effective FRW-description, such that the direction-dependence of the modes is negligible to zeroth order. Secondly, the eigenmodes in a closed universe are discrete – the spectrum shown here is, strictly speaking, a continuous approximation to the underlying discrete spectrum. It is essentially the direction-averaged power spectrum that is an enveloping function to the true quantised spectrum.

The spectrum exhibits a sharp cutoff at low k , which is a consequence of the quantity $H^2/\dot{\phi}$ turning over in the range $t \approx 9.5 - 10.5$ (which is not the case in conventional flat FRW models with straightforward power laws). Such an exponential cutoff of the form

$$\mathcal{P}_{\mathcal{R}}(k) = a(1 + b \ln(k))(1 - \exp(c(\ln(k) + d))) \quad (61)$$

has in fact been argued for on phenomenological grounds by Efstathiou [58]. Indeed, our predictions agree rather well with this proposed exponential cutoff, cf. the grey line in Figure 5. It

is intriguing that our model fits phenomenological predictions, and, in particular, this could account for the observed dip at low ℓ in the CMB power spectrum. From the power law part of the spectrum, we can extract the spectral index as $n_s = 0.975$, which is also broadly in agreement with observations [6]. The tensor spectrum is qualitatively very similar to the scalar spectrum, and yields a tensor-to-scalar ratio of approximately $r \sim 0.2$ in agreement with current constraints. Such agreement with data is encouraging. However, we must again stress that these computations are to zeroth order and more detailed computations in the anisotropic setting are needed.

The process of averaging the radii to form $R = (R_1 R_2^2)^{\frac{1}{3}}$ is effectively a map from a deformation of an FRW model back to an FRW model. To zeroth order, we could then apply all the standard machinery for FRW universes. This is certainly a very sensible way of achieving an FRW model from a Bianchi model, but is to some extent arbitrary. Looking at two other FRW models derived from our Bianchi model is instructive. One could define an FRW model simply by using each of R_1 and R_2 in turn. Of course, that will lead to problems with singularities at early times, but for the purpose of calculating fluctuation spectra one could use the numerical value of either radius in our Bianchi model just before inflation as an initial condition for an FRW model. It then turns out that in a model that has the appropriate value of R_1 as a starting point for an FRW universe at the beginning of inflation, the quantity which controls the magnitude of curvature perturbations, $H^2/\dot{\phi}$, does not turn over. The curvature spectrum in this model therefore no longer exhibits an exponential cutoff of the above mentioned form. A model based on the other radius, R_2 , however, does have a turnover similar to the one in Figure 4 and therefore an exponential cutoff in the curvature perturbation spectrum. This then explains how the unusual feature of an exponential cutoff arises via the averaging over the two differently behaved radii.

In summary, the model leads to isotropisation, necessary for compatibility with standard cosmological models at late times, as well as inflation, which accounts for structure formation. The perturbation spectrum we predict meets current constraints on the spectral index and tensor-to-scalar ratio, and offers an explanation for the dip at low ℓ in the CMB power spectrum. There is also the intriguing possibility of imprints of early oblateness on structure formation. We suggest that the universe could have been 0.2% oblate at the time when the present Hubble radius left the horizon.

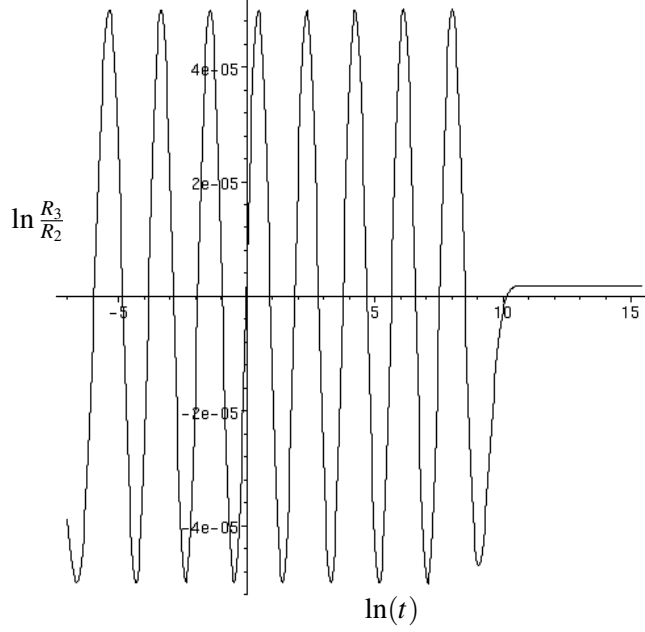


FIG. 6: Dynamics of the full triaxial Bianchi IX model: The natural logarithm of the ratio $\frac{R_3}{R_2}$ of the nearly degenerate radii is plotted as a function of log time (in Planck units).

VI. PERTURBATIONS AROUND THE AXISYMMETRIC CASE

Given the remarkable properties of this axisymmetric model, it is important to know how stable it is to perturbations. If a small fractional perturbation $R_3(t)/R_2(t) = 1 + \delta(t)$ in the initial radii evolved to universes in which $R_2(t)$ and $R_3(t)$ were vastly different, the axisymmetric case would hardly be a viable model for cosmology. There are several ways in which we can study the stability, both numerically and analytically.

Setting $R_3(t) = R_2(t)(1 + \delta(t))$ in the full triaxial equations yields the following dynamical equation for the fractional perturbation $\delta(t)$

$$\begin{aligned}
 (1 + \delta)\ddot{\delta} = & -\frac{4}{R_1^2}\delta^4 - \frac{16}{R_1^2}\delta^3 - \frac{(24R_2^2 - 4R_1^2)}{R_1^2R_2^2}\delta^2 \\
 & - \left((H_1 + 2H_2)\dot{\delta} + \frac{16R_2^2 - 8R_1^2}{R_1^2R_2^2} \right) \delta \\
 & - (H_1 + 2H_2)\dot{\delta}.
 \end{aligned} \tag{62}$$

One can either evolve this $\delta(t)$ -equation, or alternatively one could solve the full triaxial equations (19)-(20) numerically, subject to the initial fractional perturbation $\delta(0) \ll 1$.

We chose the latter approach, i.e. numerical integration starting from a point close to the Big

Bang with a very small fractional perturbation $\delta(0) = 10^{-4}$ around the biaxial cosmology considered in the previous section, keeping the other constants at their previous values. The numerical results show that as $t \rightarrow 0$ ($\ln(t) \rightarrow -\infty$) R_1 approaches zero, but the ratio of R_3/R_2 undergoes an infinite set of oscillations. (The evolution of the quantities corresponding to Figures 1 to 3 are indistinguishable from their biaxial counterparts and hence not shown again.) This is indeed what we would expect for the triaxial case (as cited previously, [37]; cf. Figure 6). However, we are interested in what happens to these oscillations at large t rather than at early times. The results show that the oscillations cease and the ratio gets frozen in around the onset of inflation. This shows that for small perturbations a steady state is eventually reached where the ratio $R_3(t)/R_2(t)$ reaches a constant value. In particular, the resulting value of $R_3(t)/R_2(t)$ differs from unity by an amount that is similar to the initial fractional perturbation. Hence the small perturbation does not lead ultimately to vastly different radii.

Note that here we mean by $t = 0$ a different time from in previous sections. Until now, $t = 0$ was naturally defined to be the time where pancaking occurs. However, perturbing and therefore going to the full triaxial equations will in general lead to an oscillatory singularity (see above, [37]). Instead, we now take $t = 0$ to mean the point where we impose the boundary conditions. These conditions are exactly the same those applied previously at the Big Bang, except that now the boundary condition for the perturbed radius R_3 is $R_3(0) \equiv R_2(0)(1 + \delta(0)) = b_0(1 + \delta(0))$.

It is worth noting that, as illustrated in Figure 6, the *ratios* of the scale factors become frozen-in. Thus, even if the values of the scale factors in each direction differ slightly, the Hubble functions $H_i(t)$ in each direction will be equal. This then raises the question as to whether such a situation would be observationally distinguishable from an FRW universe at all. It does not seem to be in the flat case, but the fact that closed and open universes have an absolute distance scale associated with them via the curvature scale seems to suggest that it would be detectable. These considerations will also be described in future work.

In fact the behaviour of the small perturbations around the biaxial case is reminiscent of the evolution of the conventional curvature perturbations generated from quantum fluctuations considered earlier. These oscillate on subhorizon scales but get frozen in on superhorizon scales. They are often regarded as mini-FRW-universes that are locally over- (or under-) dense and evolve in another FRW-background model. It seems obvious that these can in general be anisotropic, so that Bianchi models, in particular Bianchi IX, might be good for describing cosmological perturbations even when the background model is strictly Friedmann-Robertson-Walker. The different

behaviour on subhorizon and superhorizon scales is normally explained by saying that subhorizon scales describe causally connected regions where ‘there is time for local differences in matter distribution to affect the physics’. Superhorizon scales, however, are causally disconnected and frozen in. The cosmologically relevant scales that were previously subhorizon are stretched to superhorizon scales by inflation, and are now slowly coming back into the horizon. Therefore it is only natural to think of the perturbations in the Bianchi model in the same way – as stretched to superhorizon scales by inflation and frozen in.

We can make this empirical connection slightly more quantitative. Consider the evolution of a curvature perturbation associated with a comoving wavenumber k in a flat FRW-universe [54]. (Note that this is an excellent approximation for our model after the start of inflation.) This is given by

$$\ddot{\zeta}_k + \left(\frac{\dot{\phi}^2}{H} + 2\frac{\ddot{\phi}}{\dot{\phi}} + 3H \right) \dot{\zeta}_k + \frac{k^2}{R^2} \zeta_k = 0. \quad (63)$$

This equation is of harmonic oscillator form. However, amplitude and frequency are time-dependent. Thus it is reasonable that, in general, the motion will be oscillatory. At late times (after inflation), however, the effects of the scalar field driving inflation are negligible and the Hubble radius is large, so overall the damping term is negligible. Also the size of the universe is then large, so that the equation basically reduces to $\ddot{\zeta}_k = 0$. Thus at late times the perturbation gets frozen in.

Now consider perturbations around the biaxial case (62) in the late-time, isotropic limit $H_i = H$, $R_i = R$. This yields

$$\ddot{\delta} + 3H\dot{\delta} + \frac{8}{R^2}\delta = 0. \quad (64)$$

Thus the two different kinds of perturbation actually obey very similar equations. They are practically of the same form when the effect of the scalar field is negligible (after inflation). The fact that the terms involving the respective function and its first derivative are suppressed by the expansion of the universe explains why both types of oscillation become frozen-in eventually. From the equations, we would, however, expect the evolution of δ to exhibit much less variation of amplitude and period with time, which is indeed what is observed numerically. Hence, at the level of the dynamical equations, it is reasonable that the two different sorts of perturbation look so similar. The deeper question of why they should obey such similar equations will be considered in a future work.

One could, alternatively, argue that the more natural variable to consider is the fractional per-

turbation in the Hubble functions, rather than the radii. We choose to parameterise this fractional perturbation in an analogous way as $H_3(t) = H_2(t)(1 + h(t))$. Its evolution is governed by the equation

$$\begin{aligned} \dot{h} = & -\frac{1}{2}(H_1 + H_2)h^2 \\ & -\frac{1}{2}\left(2H_1H_2 + H_2^2 + 3\frac{R_1^2}{R_2^2R_3^2} + 3\frac{R_3^2}{R_1^2R_2^2} - 5\frac{R_2^2}{R_1^2R_3^2} + 2\frac{1}{R_1^2} + 2\frac{1}{R_3^2} - 6\frac{1}{R_2^2} - \kappa p + \Lambda\right)\frac{h}{H_2} \\ & -4\left(\frac{R_3^2}{R_1^2R_2^2} - \frac{R_2^2}{R_1^2R_3^2} + \frac{1}{R_3^2} - \frac{1}{R_2^2}\right)\frac{1}{H_2}. \end{aligned} \quad (65)$$

From this equation it can be seen that, in fact, an expansion in which two axes have the same Hubble function is favoured and stable: for a small initial fractional perturbation the terms in powers of h are negligible, and the constant term vanishes when $R_2 = R_3$, which implies that $h = 0$ and, from (65), $\dot{h} = 0$. This further supports the claim that this biaxial model is stable and hence a viable and interesting cosmological model.

VII. BOUNCE SOLUTION

In addition to the odd-parity, pancaking solution that we have discussed so far, there also exists an even-parity, bouncing solution to the biaxial evolution equations (25–28). In this solution, all radii are finite at the Big Bang and go smoothly through into a pre-Big Bang phase. The series solution ansatz akin to (30) is even under parity

$$\begin{aligned} R_1(t) &= a_0 + a_2t^2 + a_4t^4 + \dots \\ R_2(t) = R_3(t) &= b_0 + b_2t^2 + b_4t^4 + \dots \\ \phi(t) &= f_0 + f_2t^2 + f_4t^4 + \dots \end{aligned} \quad (66)$$

In contrast to the previous series solution, the Friedmann constraint is not automatically satisfied, and leads to an additional constraint determining a_0 in terms of b_0 , f_0 , etc. Figure 7 shows the basic dynamics of this model. Both radii are constant and non-zero at the Big Bang, and the effect of the scalar field is again to inflate and isotropise the universe. For considerations concerning a presentation in terms of shear and curvature, see the appendix. This model might be interesting in its own right, and further details will be presented elsewhere. For previous work on bouncing solutions and their likelihood see, for example, [59, 60].

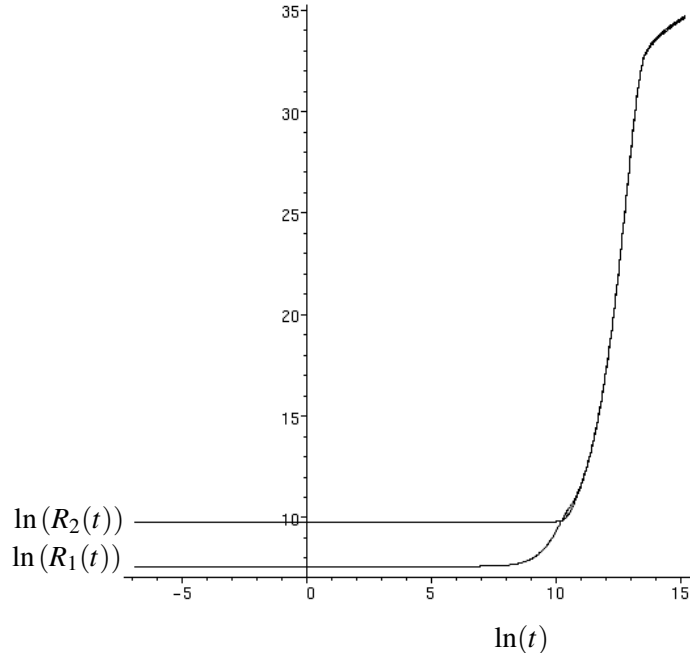


FIG. 7: Dynamics of the bouncing solution: evolution of the logarithm of the scale factors R_1 and R_2 in Planck lengths l_p versus log time (t in units of Planck time t_p).

VIII. CONCLUSIONS

We have presented a novel scenario in which the effect of a scalar field and biaxial Bianchi IX geometry is to render the Big Bang much better behaved. Physical quantities remain finite at the Big Bang, and there is no curvature singularity at the time of pancaking. This is in contrast with singularities in flat and open FRW-models, and essential singularities in the full triaxial Bianchi IX case. In addition, the investigation of the behaviour of geodesics suggests that some physical observers can cross over and move smoothly into a pre-Big Bang phase. Some observers, however, may not be able to cross and this would appear to make the model incomplete, with the pancake being a quasiregular singularity (the type that also occurs in Taub-NUT). However, in the light of periodic identification of angular coordinates on the 3-sphere and the fact that the winding direction is the collapsing dimension, this might not be such a problem. The model also exhibits stability under sufficiently small perturbations around biaxiality. Though the model isotropises at late times, we show that structure on the largest scales could in fact stem from a time at which the universe was significantly anisotropic. Such behaviour is very desirable for a satisfactory cosmological model, as a closed universe can be matched to the observed asymptotic de Sitter phase of

Λ -domination, whilst the scalar field can drive isotropisation, so as to account for the observed degree of isotropy of the universe, and inflation, thought to be needed in order to explain the observed perturbation spectrum. We predict a spectral index and a tensor-to-scalar ratio compatible with current constraints, as well as a dip at low multipoles of the CMB power spectrum, which is consistent with an exponential cutoff that has also been argued for on phenomenological grounds. We explain the apparent qualitative similarity between the two very different kinds of perturbations, namely curvature perturbations and perturbations around biaxiality, from their evolution equations. A separate, bouncing solution is also presented, and will be considered in more detail elsewhere. A more thorough analysis of many subtleties of the model, in particular the issue of geodesic completeness and a detailed comparison with Taub-NUT is in preparation.

Acknowledgments

We thank the referee for their very useful suggestions. We also thank John Barrow, Sylvain Bréchet, Carlo Contaldi, Leonardo Fernández-Jambrina, Cyril Pitrou, Paolo Salucci, Subir Sarkar, Jiro Soda and others for helpful comments and for pointing out relevant references. PPD is grateful for support through an STFC (formerly PPARC) studentship.

APPENDIX: DYNAMICS IN THE 3 + 1 COVARIANT APPROACH

Here we use the timelike eigenvector $u_\mu = [1, 0, 0, 0]$ of the scalar field energy-momentum tensor as the ‘velocity field’ to perform a 3 + 1 split (see, for example, [61]) in order to present the equations (25)-(28) in a different parametrisation, which might be convenient for other applications, and in particular separates more clearly the contributions of curvature and shear. Many quantities in the general 3 + 1 approach vanish for our particular case, such as the peculiar acceleration, vorticity and anisotropic stress. The dynamical equations can therefore be recast simply in terms of the averaged scale factor, i.e. the volume expansion,

$$R \equiv (R_1 R_2 R_3)^{\frac{1}{3}} \rightarrow (R_1 R_2^2)^{\frac{1}{3}}, \quad (\text{A.1})$$

its associated Hubble factor,

$$3H = H_1 + H_2 + H_3 \rightarrow H_1 + 2H_2, \quad (\text{A.2})$$

and the shear scalar σ^2

$$\sigma^2 = \frac{1}{6} \left[(H_1 - H_2)^2 + (H_2 - H_3)^2 + (H_3 - H_1)^2 \right] \rightarrow \frac{1}{3} (H_1 - H_2)^2, \quad (\text{A.3})$$

where the expressions on the right denote the biaxial limit. The shear tensor $\sigma_{\mu\nu}$ is defined as $\sigma_{\mu\nu} \equiv \tilde{\nabla}_{\langle\mu} u_{\nu\rangle}$, where $\tilde{\nabla}$ is the fully orthogonally projected covariant derivative (for details, see [61]). The shear tensor has three spacelike eigenvectors characterised in a coordinate-free way by their eigenvalues. In the biaxial case, for instance, one is $\frac{2}{3}(H_1 - H_2)$, whereas the other two are degenerate and have the value $-\frac{1}{3}(H_1 - H_2)$, whence the above shear scalar follows from $\sigma^2 \equiv \frac{1}{2}\sigma_{\mu\nu}\sigma^{\mu\nu}$.

In this parametrisation, the Raychudhuri equation assumes the form

$$3\dot{H} + 3H^2 = -\frac{\kappa}{2}(\rho + 3p) - 2\sigma^2 + \Lambda. \quad (\text{A.4})$$

The Friedmann equation can be reexpressed as

$$H^2 = \frac{\kappa\rho}{3} + \frac{\sigma^2}{3} + \frac{\Lambda}{3} + \frac{R^{(3)}}{6}, \quad (\text{A.5})$$

where $R^{(3)}$ is the Ricci scalar of the orthogonal 3-spaces, which here evaluates to

$$R^{(3)} = 2 \left(\frac{R_1^2}{R_3^2 R_2^2} + \frac{R_2^2}{R_3^2 R_1^2} + \frac{R_3^2}{R_1^2 R_2^2} - \frac{2}{R_1^2} - \frac{2}{R_2^2} - \frac{2}{R_3^2} \right) \rightarrow \frac{2}{R_2^2} \left(\frac{R_1^2}{R_2^2} - 4 \right). \quad (\text{A.6})$$

This uncovers the geometric significance of the corresponding term in the triaxial Friedmann equation (21). We also find that the $-H_1 H_2 - H_2 H_3 - H_3 H_1$ term just corresponds to $3H^2 - \sigma^2$ (up to sign), and $3H^2 + 2\sigma^2 = H_1^2 + H_2^2 + H_3^2$. This also correctly reduces to the standard FRW results in the isotropic limit, as do the equations themselves. The usual shear propagation for vanishing peculiar acceleration and anisotropic stress is

$$\dot{\sigma}_{\langle\mu\nu\rangle} + 3H\sigma_{\mu\nu} = R_{\mu\nu}^{(3)} - \frac{1}{3}h_{\mu\nu}R^{(3)}, \quad (\text{A.7})$$

where $R_{\mu\nu}^{(3)}$ and $R^{(3)}$ are the Ricci tensor and scalar of the orthogonal 3-spaces, respectively. However, in the biaxial case, the evolution equation for the shear scalar suffices, and turns out to be

$$\dot{\sigma} + 3H\sigma = \frac{1}{2\sigma}R_{\mu\nu}^{(3)}\sigma^{\mu\nu} = -\frac{4}{\sqrt{3}R_2^2} \left(\frac{R_1^2}{R_2^2} - 1 \right). \quad (\text{A.8})$$

This can be seen upon contracting (A.7) with $\sigma^{\mu\nu}$ and noting that $\dot{\sigma}_{\langle\mu\nu\rangle}\sigma^{\mu\nu} = \dot{\sigma}_{\mu\nu}\sigma^{\mu\nu} = \frac{1}{2}(\sigma_{\mu\nu}\sigma^{\mu\nu})' = 2\sigma\dot{\sigma}$, i.e. since one is contracting with something purely spatial, the projection

onto the 3-spaces prior to the contraction does not change the result. Furthermore, the term involving the Ricci scalar of the 3-surfaces just extracts the trace of the shear, which vanishes by definition.

The equation of motion for the scalar field just retains its usual Klein-Gordon form

$$m^2\phi + 3H\dot{\phi} + \ddot{\phi} = 0. \quad (\text{A.9})$$

Using the series solution (30) for the pancaking solution, we find that

$$R(t) = (R_1 R_2^2)^{\frac{1}{3}} \propto t^{\frac{1}{3}}, \quad (\text{A.10})$$

to lowest order in t . By the same token, the shear scalar behaves as

$$\sigma^2 = \frac{1}{3} \left(\frac{R_2}{R_1} \right)^2 \left(\frac{d}{dt} \left(\frac{R_1}{R_2} \right) \right)^2 = \frac{1}{3} t^{-2} + O(1) \propto R^{-6} + O(1), \quad (\text{A.11})$$

as might be expected from the naive form of equation (A.8) $\dot{\sigma} + 3H\sigma = 0$, which holds in the better-known flat and isotropic limits. Note that this does not contradict equation (A.8). The lowest order term in the series expansion for σ is $\sigma \propto H_1(t) \propto \frac{1}{t}$ which results in $\dot{\sigma} \propto -\frac{1}{t^2}$ to lowest order. This happens to cancel exactly the $\frac{1}{t^2}$ term resulting from the product of $\sigma \propto \frac{1}{t}$ and $H(t) \propto H_1(t) \propto \frac{1}{t}$, such that the leading order of the combined $\dot{\sigma} + 3H\sigma$ is actually the constant that is the leading term on the right hand side of (A.8). Also note that the approximate time-dependence of the shear scalar does not involve any of the parameters that need to be set in our model, which is remarkable. The curvature of the orthogonal 3-space is constant across the pancake

$$R^{(3)} = -\frac{8}{b_0^2}, \quad (\text{A.12})$$

whereas the shear diverges, as shown. This means that in a pancaking Bianchi IX model the shear will always dominate over the curvature at early enough times, such that the model is actually well approximated by a Bianchi I model, though they are of course different topologically.

Figure 8 depicts the motion of the pancaking model through the shear-curvature-parameter space. Note that since the shear diverges at the time of pancaking we have chosen to plot the model's trajectory in the $(\ln \sigma, R^{(3)})$ -space rather than the $(\sigma, R^{(3)})$ -space itself (which will be appropriate for the bouncing solution). At early times, the shear diverges, whereas the curvature is constant, which accounts for the divergence in the top left of the plot corresponding to the time of pancaking. During inflation the curvature is quickly driven to zero and the universe isotropises i.e. the shear vanishes, which accounts for the late-time behaviour in the bottom right part.

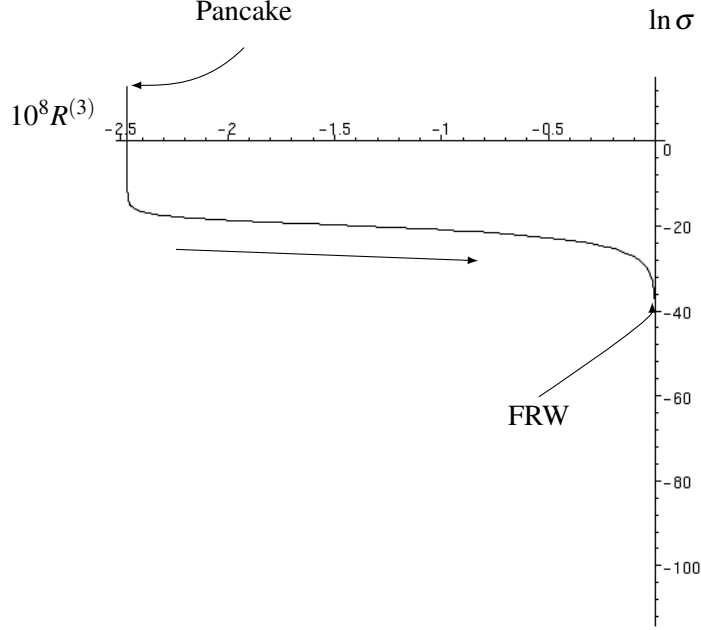


FIG. 8: $(\sigma, R^{(3)})$ -trajectory for the pancaking solution: evolution of the logarithm of the shear versus the Ricci scalar of the orthogonal 3-surfaces.

Similarly, for the bouncing solution (66), we find that

$$R(t) \propto \text{constant}, \quad (\text{A.13})$$

and also the shear is constant (in fact vanishes) to first order

$$\sigma^2 = \frac{4}{3} \left(\frac{a_2}{a_0} - \frac{b_2}{b_0} \right)^2 t^2 \approx 0, \quad (\text{A.14})$$

as might be expected, since all the dynamical variables have an extremum at the bounce. The Ricci scalar of the 3-surfaces is also constant

$$R^{(3)} = \frac{2}{b_0^2} \left(\frac{a_0^2}{b_0^2} - 4 \right). \quad (\text{A.15})$$

This means that for a bouncing model, contrary to the pancaking case, the curvature will generically dominate over the shear at the bounce.

Figure 9 shows the motion of the bouncing model through the shear-curvature-parameter space. At early times, the shear vanishes, and likewise at late times. The shear therefore peaks at intermediate times in the bouncing model. The curvature shows the same behaviour as the pancaking solution in that it is constant at early times and the model is then driven to flatness during inflation.

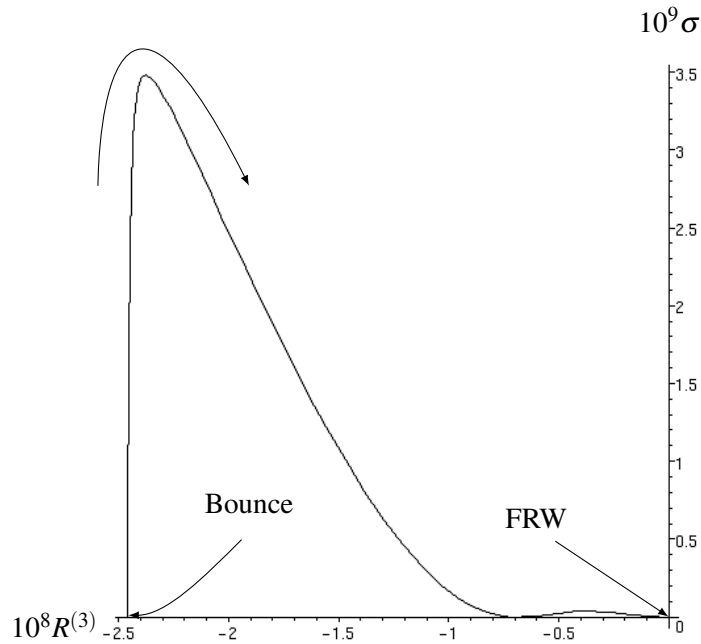


FIG. 9: $(\sigma, R^{(3)})$ -trajectory for the bouncing solution: evolution of the shear versus the Ricci scalar of the orthogonal 3-surfaces.

So we can identify the bottom left hand area of the plot with the bounce, where the curvature is maximal and the shear vanishes. The shear then peaks at intermediate times whilst the curvature decreases. The bottom right hand corner again corresponds to the late-time evolution which is driven to isotropy and spatial flatness. Note that in both cases the numerical value of the initial curvature is exactly what we expect for the chosen parameter values. They appear to be nearly the same since for the particular models chosen here $a_0 \ll b_0$.

-
- [1] T. S. Pereira, C. Pitrou, and J.-P. Uzan, JCAP **9**, 6 (2007), 0707.0736.
 - [2] C. Pitrou, T. S. Pereira, and J.-P. Uzan, JCAP **4**, 4 (2008), 0801.3596.
 - [3] A. Gümürkçüoğlu, C. Contaldi, and M. Peloso, JCAP **11**, 005 (2007).
 - [4] A. Lasenby and C. Doran, Phys. Rev. D **71**, 063502 (2005).
 - [5] A. Lasenby and C. Doran, AIP conf. proc. **736**, 53 (2004).
 - [6] D. Spergel et al., ApJS **170**, 377408 (2007).

- [7] A. V. Toporensky and V. O. Ustiansky, gr-qc/9907047 (1999).
- [8] S. Fay and T. Lehner, *Gen. Rel. Grav.* **37**, 1097 (2005).
- [9] A. Coley and M. Goliath, *Phys. Rev. D* **62**, 043526 (2000).
- [10] C. W. Misner, *Phys. Rev. Lett.* **22**, 1071 (1969).
- [11] B. A. Belinsky, I. M. Khalatnikov, and E. M. Lifshitz, *JETP* **62**, 1606 (1972).
- [12] B. A. Belinsky, I. M. Khalatnikov, and E. M. Lifshitz, *JETP* **60**, 1969 (1971).
- [13] G. F. R. Ellis and M. A. H. MacCallum, *Commun. Math. Phys.* **12**, 108 (1969).
- [14] I. D. Novikov and Y. B. Zel'dovich, *Annu. Rev. Astro. Astrophys.* **11**, 387 (1973).
- [15] G. F. R. Ellis, *Gen. Relativ. Gravit.* **38**, 1003 (2006).
- [16] J. M. Heinzle and C. Uggla, ArXiv e-prints (2009), 0901.0776.
- [17] J. M. Heinzle and C. Uggla, ArXiv e-prints (2009), 0901.0806.
- [18] J. M. M. Senovilla, *Phys. Rev. Lett.* **64**, 2219 (1990).
- [19] E. Ruiz and J. M. M. Senovilla, *Phys. Rev. D* **45**, 1995 (1992).
- [20] F. J. Chinea, L. Fernández-Jambrina, and J. M. M. Senovilla, *Phys. Rev. D* **45**, 481 (1992).
- [21] L. Fernández-Jambrina and L. M. González-Romero, *Phys. Rev. D* **66**, 024027 (2002).
- [22] D. S. Goldwirth and T. Piran, *Physics Reports* **214**, 223 (1992).
- [23] S. Kanno, M. Kimura, J. Soda, and S. Yokoyama, *JCAP* **8**, 34 (2008), 0806.2422.
- [24] B. Himmetoglu, C. R. Contaldi, and M. Peloso (2008), 0809.2779.
- [25] L. Bianchi, *Mem. della Soc. It. delle Scienze (detta dei XL)* (3) **11**, 267 (1897).
- [26] A. H. Taub, *Ann. Math.* **53**, 472 (1951).
- [27] O. Heckmann and E. Schücking, *Gravitation* (Wiley, New York, 1962).
- [28] J. Wainwright and G. Ellis, *Dynamical Systems in Cosmology* (Cambridge University Press, 1997).
- [29] C. B. Collins and S. W. Hawking, *The Astrophysical Journal* **180**, 317 (1973).
- [30] G. F. R. Ellis and M. A. H. MacCallum, *Commun. Math. Phys.* p. 1072 (1968).
- [31] S. W. Hawking and G. F. R. Ellis, *The Large Scale Structure of Space-Time* (Cambridge University Press, 1973).
- [32] H. Stephani et al., *Exact Solutions to Einstein's Field Equations, 2nd edition* (Cambridge University Press, 2003).
- [33] C. Doran, A. Lasenby, and J. Lasenby, *Uncertainty in Geometric Computations* (Kluwer Academic Publishers, Boston, 2002), chap. Conformal Geometry, Euclidean Space and Geometric Algebra, pp. 41–58.

- [34] C. Doran and A. N. Lasenby, *Geometric Algebra for Physicists* (Cambridge University Press, 2003).
- [35] J. D. Barrow, *Nature* **272**, 211 (1978).
- [36] J. D. Barrow, *Nucl. Phys. B* **296**, 697 (1988).
- [37] M. P. Ryan and L. C. Shepley, *Homogeneous Relativistic Cosmologies* (Princeton University Press, 1975).
- [38] K. Becker, M. Becker, and J. H. Schwarz, *String Theory and M-Theory* (Cambridge University Press, 2007).
- [39] T. Ortín, *Gravity and Strings* (Cambridge University Press, 2004).
- [40] C. V. Johnson, *D-Branes* (Cambridge University Press, 2003).
- [41] D. A. Konkowski, T. M. Helliwell, and L. C. Shepley, *Phys. Rev. D* **31**, 1178 (1985).
- [42] D. A. Konkowski and T. M. Helliwell, *Phys. Rev. D* **31**, 1195 (1985).
- [43] G. F. R. Ellis and B. G. Schmidt, *Gen. Rel. Grav.* **8**, 915 (1977).
- [44] D. A. Konkowski and T. M. Helliwell, in *The Tenth Marcel Grossmann Meeting. On recent developments in theoretical and experimental general relativity, gravitation and relativistic field theories*, edited by M. Novello, S. Perez Bergliaffa, and R. Ruffini (2005), pp. 1829–+.
- [45] C. Gordon and N. Turok, *Phys. Rev. D* **67**, 123508 (2003).
- [46] R. M. Wald, *Phys. Rev. D* **28**, 2118 (1983).
- [47] J. D. Barrow, *Phys. Lett. B* **187**, 12 (1987).
- [48] Y. Kitada and K. I. Maeda, *Phys. Rev. D* **45**, 1416 (1992).
- [49] Y. Kitada and K. I. Maeda, *Class. Quantum Grav.* **10**, 703 (1993).
- [50] P. Salucci and R. Fabbri, *Nuovo Cimento B Serie* **77**, 62 (1983).
- [51] A. R. Liddle and D. H. Lyth, *Cosmological Inflation and Large Scale Structure* (Cambridge University Press, 2000).
- [52] J.-P. Uzan, U. Kirchner, and G. F. R. Ellis, *MNRAS* **344**, L65 (2003).
- [53] A. A. Starobinsky, *Cosmoparticle Physics* (Frontiers, 1996), chap. Spectrum of initial perturbations in open and closed universes, p. 43.
- [54] M. P. Hobson, G. P. Efstathiou, and A. N. Lasenby, *General Relativity: An Introduction for Physicists* (Cambridge University Press, 2006).
- [55] K. Dimopoulos, D. H. Lyth, and Y. Rodríguez (2008), 0809.1055.
- [56] S. Gratton, J. Khoury, P. J. Steinhardt, and N. Turok, *Phys. Rev. D* **69**, 103505 (2004).
- [57] J. K. Erickson, S. Gratton, P. J. Steinhardt, and N. Turok, *Phys. Rev. D* **75**, 123507 (2007).

- [58] G. Efstathiou, MNRAS **343**, L95 (2003).
- [59] J. D. Barrow and R. A. Matzner, Phys. Rev. D **21**, 336 (1980).
- [60] F. T. Falciano, M. Lilley, and P. Peter, Phys. Rev. D **77**, 083513 (2008), 0802.1196.
- [61] G. F. R. Ellis and H. van Elst, *Cosmological models*, Cargse Lectures (1998).